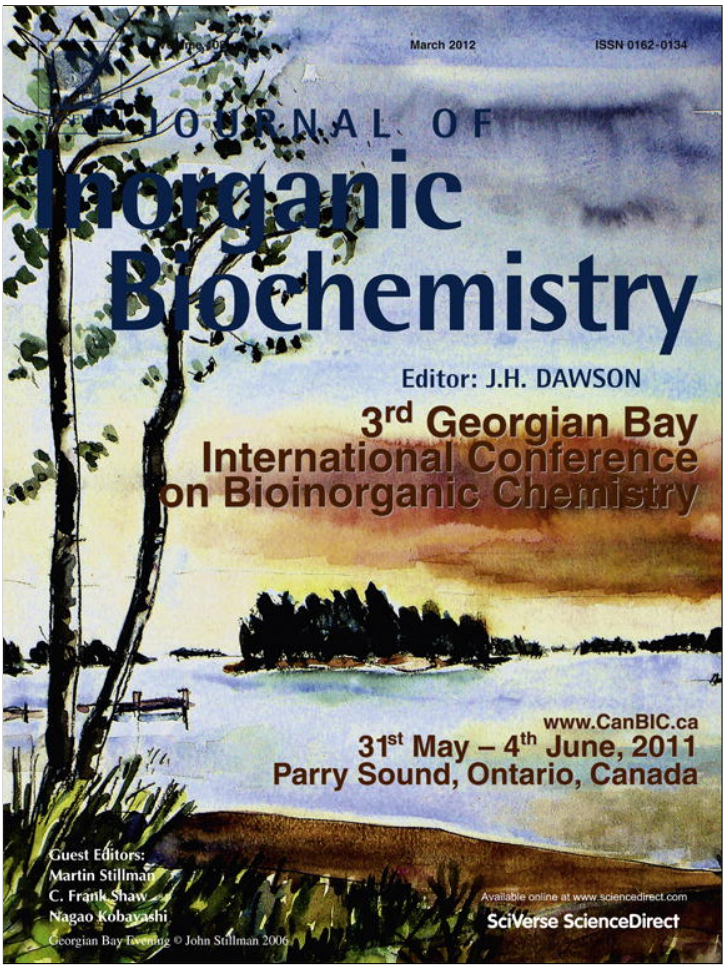

Journal of Inorganic Biochemistry 108 (2012) 1–7

Contents lists available at SciVerse ScienceDirect

Journal of Inorganic Biochemistry

journal homepage: www.elsevier.com/locate/jinorgbio

Novel Pt(II) and Pd(II) complexes with polyamine analogues: Synthesis and vibrational analysis

T.M. Silva [a,b,c], S. Oredsson [b], L. Persson [c], P. Woster [d], M.P.M. Marques [a,e,*]

[a] Research Unit "Molecular Physical Chemistry", University of Coimbra, Portugal
[b] Department of Biology, University of Lund, Sweden
[c] Department of Experimental Medical Science, University of Lund, Sweden
[d] Department of Pharmaceutical and Biomedical Sciences, Medical University of South Carolina, SC, USA
[e] Department of Life Sciences, Faculty of Science and Technology, University of Coimbra, Portugal

ARTICLE INFO

Article history:
Received 26 August 2011
Received in revised form 10 November 2011
Accepted 23 November 2011
Available online 3 December 2011

Keywords:
Modified polyamines
Pt(II) / Pd(II) complexes
Raman spectroscopy
Infrared spectroscopy
Anticancer

ABSTRACT

A vibrational spectroscopy study (infrared and Raman) is reported for the biogenic polyamine analogues norspermidine (NSpd), N^1,N^{11}-bis(ethyl)norspermine (BENSpm) and N^1-cyclo-propylmethyl-N^{11}-ethylnorspermine (CPENSpm), as well as for their newly synthesised Pt(II) and Pd(II) complexes. Attending to the potential antineoplastic properties of this kind of systems, their full conformational characterization is essential for understanding the molecular basis of their cytotoxic activity and the mechanisms through which they are transported into the cell. The *all-trans* geometry was found to be favoured for all the alkylated polyamines, in their totally protonated state, while their polynuclear complexes presented a stable geometry very similar to that previously obtained for the analogous chelates with spermidine (M_3Spd_2) and spermine (M_2Spm), comprising two or three cisplatin-like (MCl_2NH_2) moieties.

1. Introduction

Biogenic polyamines (PA's) – putrescine (Put, $H_2N(CH_2)_4NH_2$), spermidine (Spd, $H_2N(CH_2)_3NH(CH_2)_4NH_2$) and spermine (Spm, $H_2N(CH_2)_3NH(CH_2)_4NH(CH_2)_3NH_2$) – are ubiquitous in cells of higher organisms, and essential for their growth and differentiation through tightly regulated processes [1,2]. Because of absolute polyamine requirement for cell proliferation, coupled to the positive correlation between polyamine levels and tumour growth, polyamines are regarded as a crucial target for anticancer treatment [3]. Numerous studies have focused on PA depletion by using synthetic antagonists, or by modulating specific enzymes associated to polyamine metabolism or degradation. Moreover, the chemotherapeutic effect of conventional chemotherapeutic agents may be assisted by this PA depletion in the tumour and host tissues, through the combined use of polyamine analogues which can even induce a synergistic effect with standard DNA-reactive cytotoxic drugs [4].

Modified biogenic polyamines, in particular, have been shown to affect the regulatory paths associated to PA's biosynthesis, catabolism and transport, through a Trojan horse mechanism: the cell recognises these polyamine analogues as natural polyamines and they are promptly taken up and accumulated to high levels, thus stimulating PA catabolism while inhibiting the cellular uptake of biogenic PA's. Thus, the cell becomes depleted of these polyamines while being filled with the analogues which cannot take over their function [5]. Numerous PA analogues have lately been synthesised in view of their use in cancer chemotherapy [6] – either symmetrically or unsymmetrically alkylated (*e.g.* at the terminal nitrogens), conformationally restricted, or varying in the N-to-N alkyl bridges – and some of them have shown exceptional efficacy in animal tumour models coupled to surprisingly low toxicity in humans. The ethyl-substituted spermine analogue BENSpm (N^1,N^{11}-bis(ethyl) norspermine), for instance, has shown a significant activity (both *in vitro* and *in vivo*) against human breast cancer cells [7,8], and is currently under Phase II of clinical trials [9]. This compound has also been found to exhibit a synergistic inhibitory effect on breast cancer cell proliferation in combination with 5-fluorouracil and paclitaxel [10], possibly through a novel antioestrogenic mechanism (*via* the oestrogen receptor α).

Additionally, this type of linear alkylpolyamines is suitable ligands for metal ions such as Pt(II) and Pd(II), yielding complexes (namely polynuclear chelates) that were found to act as promising antineoplastic agents through a non-conventional (long-range interstrand) interaction with DNA, often displaying a higher efficacy than standard

* Corresponding author at: Department of Life Sciences, Faculty of Science and Technology, University of Coimbra, Ap. 3046, 3001-401 Coimbra, Portugal. Tel.: +351 239826541, fax : +351 239854448.
E-mail address: pmc@ci.uc.pt (M.P.M. Marques).

0162-0134/$ – see front matter © 2011 Elsevier Inc. All rights reserved.
doi:10.1016/j.jinorgbio.2011.11.021

drugs (*e.g.* cisplatin, *cis*-$Pt(NH_3)_2Cl_2$) [11,12]. However, although the transport, cellular uptake and activity of both the PA analogues and their metal chelates are known to be strongly dependent on their structural characteristics, these highly sensitive structure–activity relationships (SAR's) are very poorly known, which urges for a detailed analysis of this kind of systems at the molecular level.

Furthermore, in view of the promising results already obtained by the authors for bi- and trinuclear Pt(II) and Pd(II) chelates of spermidine and spermine regarding their interaction with DNA and antineoplastic properties [13–21], the present study on similar complexes with analogous PA's is of the utmost relevance with a view to optimize the anticancer activity of this kind of PA-based agents, in the light of their structural profile.

Therefore, this work has a twofold objective: i) the study of several modified polyamines by vibrational spectroscopic methods – Fourier transform infrared (FTIR) and Raman – coupled to quantum mechanical calculations, which, to the best of the authors' knowledge, have never been reported for these analogues—NSpd (norspermidine, $H_2N(CH_2)_3NH(CH_2)_3NH_2$), BENSpm ($N^1$,$N^{11}$-bis(ethyl)norspermine, $(CH_3CH_2)HN(CH_2)_3NH(CH_2)_3NH(CH_2)_3NH(CH_3CH_2)$) and CPENSpm ($N^1$-cyclopropyl-methyl-$N^{11}$-ethylnorspermine, $(CH_2C_3H_5)HN(CH_2)_3$-$NH(CH_2)_3NH(CH_2)_3NH(CH_3CH_2)$ (Fig. 1); ii) the synthesis of new Pt(II) and Pd(II) complexes with NSpd and BENSpm, and their structural analysis by vibrational spectroscopy coupled to quantum mechanical calculations. The results will be compared and interpreted in the light of extensive spectroscopic and theoretical data previously obtained by the authors on the corresponding biogenic polyamines and their Pt(II) and Pd(II) chelates [22–31]. The influence of factors such as the type and number of metal centres, the nature of the ligands and the coordination pattern will be assessed. The knowledge thus gathered will be correlated with the corresponding biological profile – cytotoxicity and interference with polyamine homeostasis – assessed in a parallel study towards human breast cancer cells [T.M. Silva, S. Oredsson, L. Persson and M.P.M. Marques, manuscript in preparation], thus allowing to determine the molecular basis of this biological activity.

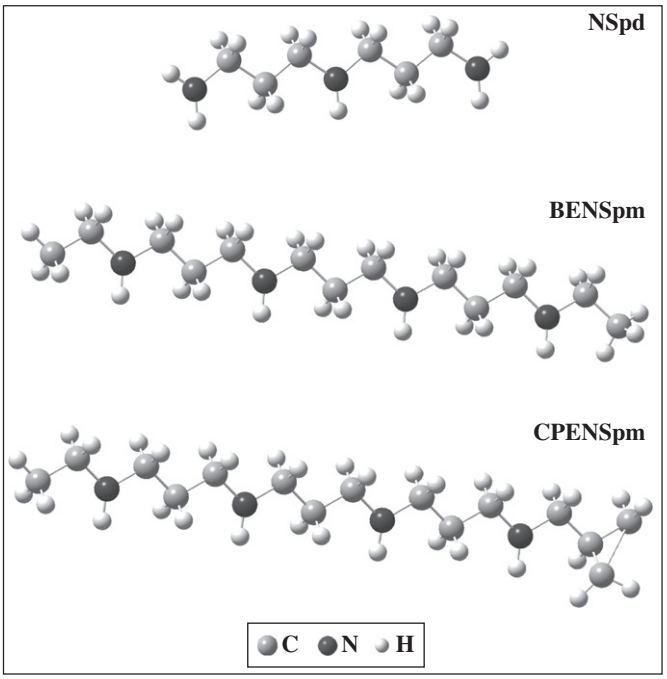

Fig. 1. Most stable structures calculated (B3LYP/6-31G**) for NSpd, BENSpm and CPENSpm.

2. Experimental procedure

2.1. Chemicals

K_2PtCl_4 (>99.9%), K_2PdCl_4 (98%) and NSpd trihydrochloride (98%) were purchased from Sigma-Aldrich Chemical Co. (Sintra, Portugal). All chemicals and solvents were reagent grade and were used without further purification.

The PA analogues BENSpm tetrahydrochloride and CPENSpm tetrahydrobromide were made available by Dr Patrick Woster.

2.2. Synthesis

Novel Pt(II) and Pd(II) complexes with PA analogues were synthesised, according to optimised procedures based on previously reported methods for similar compounds (Pt(II) and Pd(II) chelates with biogenic polyamines [21,32,33]). The analogues used were either symmetrically or unsymmetrically substituted at the terminal nitrogens (BENSpm and CPENSpm, respectively), or alkylpolyamines varying in the N-to-N methylene bridges relative to the biogenic compound (NSpd) (Fig. 1). The chelates studied along this work were $(MCl_2)_3(NSpd)_2$ (M = Pt(II) and Pd(II)), $(PdCl_2)_2$(BENSpm) and $(PtCl_2)_2$(CPENSpm).

$(PdCl_2)_3(NSpd)_2$ and $(PdCl_2)_2$(BENSpm): Briefly, 2 mmol of K_2PdCl_4 was dissolved in a minimal amount of water, and an aqueous solution containing 3 or 1 mmol of the ligand (NSpd or BENSpm, respectively) was added dropwise under continuous stirring, the pH having been adjusted to *ca.* 8 immediately after addition of the polyamine. After about 5–6 h stirring the solution was left to stand overnight. A yellow powder of the complex was obtained, which was filtered and washed repeatedly with cold acetone and ethanol. Yield: $(PdCl_2)_3(NSpd)_2$—81.2%; $(PdCl_2)_2$(BENSpm)—88.6%.

$(PtCl_2)_3(NSpd)_2$ and $(PtCl_2)_2$(CPENSpm). For the synthesis of the Pt(II) complexes a similar protocol was followed, starting from a solution containing 3 or 1 mmol of the ligand (NSpd or CPENSpm, respectively) added (dropwise, under stirring) to a concentrated aqueous solution with 2 mmol of K_2PtCl_4. Upon overnight rest a yellowish powder of the complex ($(PtCl_2)_3(NSpd)_2$ or $(PtCl_2)_2$(CPENSpm)) was obtained, filtered and washed with cold acetone and ethanol. In this case, the pH was adjusted to *ca.* 8 and 12, respectively for the NSpd and CPENSpm chelates, after adding the ligand. Yield: $(PtCl_2)_3$(-Nspd)$_2$—45.7%; $(PtCl_2)_2$(CPENSpm)—66.3%.

The elemental analysis were carried out at the Central Analysis Laboratory and Chemistry Department (Mass Spectrometry Laboratory) of the University of Aveiro (Portugal) (C, N, H), and at the Elemental Analysis Laboratory of the University of Santiago de Compostela (Spain) (Pt, Pd). $(PtCl_2)_3(Nspd)_2$—calculated—C: 13.6%, H: 3.24%, N: 7.92%, Cl: 20.06%, Pt: 55.19%; found—C: 13.33%, H: 3.16%, N: 7.89%, Pt: 55.01%. $(PdCl_2)_3(Nspd)_2$—calculated—C: 18.14%, H: 4.32%, N: 10.58%, Cl: 26.78%, Pd: 40.18%; found—C: 18.10%, H: 4.20%, N: 10.32%, Pt: 39.90%. $(PdCl_2)_2$(BENSpm)—calculated—C: 26.06%, H: 5.39%, N: 9.36%, Cl: 23.67%, Pd: 35.52%; found—C: 25.88%, H: 5.10%, N: 9.13%, Pd: 35.23%. $(PtCl_2)_2$(CPENSpm)—calculated—C: 22.45%, H: 4.28%, N: 6.98%, Cl: 17.67%, Pt: 48.62; found—C: 22.03%, H: 4.12%, N: 6.77%, Pt: 48.10%.

The complexes were further characterised by vibrational spectroscopy (FTIR and Raman—see discussion below).

2.3. FTIR spectroscopy

The Fourier transform infrared (FTIR) spectra were recorded in a Bruker Optics Vertex 70 FTIR spectrometer, in the range 400–4000 cm^{-1}, using KBr discs (*ca.* 2% (*w*/*w*)), a KBr beamsplitter, and a liquid nitrogen cooled Mercury Cadmium Telluride (MCT) detector. The FTIR spectra were collected for *ca.* 75 scans, with a 2 cm^{-1} resolution. The errors in wavenumbers were estimated to be less than 1 cm^{-1}.

2.4. Raman spectroscopy

The Raman spectra were obtained for the pure compounds, at room temperature, in a triple monochromator Jobin-Yvon T64000 Raman system (focal distance 0.640 m, aperture *f*/7.5) equipped with holographic gratings of 1800 grooves mm^{-1}. The premonochromator stage was used in the subtractive mode. The detection system was a liquid nitrogen cooled non-intensified 1024×256 pixel (1″) charge coupled device (CCD) chip.

The 514.5 nm line of an Ar^+ laser (Coherent, model Innova 300-05) was used as the excitation radiation, providing *ca.* 90 mW at the sample position. A 90° geometry between the incident radiation and the collecting system was employed. The entrance slit was set to 200 μm, as well as the slit between the premonochromator and the spectrograph. Samples were sealed in Kimax glass capillary tubes of 0.8 mm inner diameter. Under the above mentioned conditions, the error in wavenumbers was estimated to be within 1 cm^{-1}.

Room temperature Fourier transform Raman (FT–Raman) spectra were obtained in an RFS 100/S Bruker spectrophotometer. The 1064 nm line provided by a Nd:YAG laser was used, yielding 200 mW at the sample position. Resolution was set at 2 cm^{-1} and a 180° geometry was employed.

2.5. Quantum mechanical calculations

The quantum mechanical calculations were performed using the GAUSSIAN 03 W programme [34] within the Density Functional Theory (DFT) approach, in order to properly account for the electron correlation effects (particularly important in this kind of systems). The widely employed hybrid method denoted by B3LYP, which includes a mixture of HF (Hartree–Foch) and DFT exchange terms and the gradient-corrected correlation functional of Lee, Yang and Parr [35,36], as proposed and parameterised by Becke [37,38], was used, along with the double-zeta split valence basis set 6-31G** [39].

Molecular geometries were fully optimised by the Berny algorithm, using redundant internal coordinates [40]: the bond lengths to within *ca.* 0.1 pm and the bond angles to within *ca.* 0.1°. The final root-mean-square (rms) gradients were always less than 3×10^{-4} hartree.$bohr^{-1}$ or hartree.$radian^{-1}$. No geometrical constraints were imposed on the molecules under study.

The harmonic vibrational wavenumbers, as well as Raman activities and infrared intensities, were also obtained, at the same theory level as the geometry optimization procedure. The widely employed scale factors of Merrick et al. [41] were used to reproduce the experimental data, leading to a quite good agreement between theoretically predicted and experimental frequencies.

3. Results and discussion

Linear alkylpolyamines, such as biogenic PA's spermidine and spermine or the presently investigated analogues, can adopt several geometries depending on the dihedral angles that determine their overall orientation, the most common ones being 60° (*gauche*), 180° (*trans*) and −60° (*gauche′*). At physiological pH, these polyamines are polycations, all their nitrogen atoms being protonated, which hinders the formation of intramolecular (N)H ··· N or (C)H ···:N hydrogen bonds, the *all-trans* conformation being energetically favoured. In these conditions, only three effects are relevant in determining conformation: intermolecular H-bonds, electrostatic and steric forces. Previous conformational analysis of α,ω-diamines ($H_2N(CH_2)_nNH_2$, $n=2$ to 10 and $n=12$), as well as of the larger spermidine (triamine) and spermine (tetramine) [42,22–27] allowed to corroborate that the *all-trans* is the predominant or even the sole conformation for this kind of totally extended polycationic molecules in the solid state. In fact, it was verified that, in the solid, intramolecular interactions are overruled by intermolecular ones. The most stable structures for the PA analogues under study – NSpd, BENSpm and CPENSpm – are represented in Fig. 1. These were obtained through quantum mechanical methods, as the lowest energy geometries among the several possible conformations calculated for each molecule.

The corresponding vibrational analysis, carried out by both FTIR and Raman, allows to corroborate these conformational preferences. Interpretation of the experimental data was assisted by the calculated geometries and corresponding vibrational pattern, a quite good agreement having been obtained in all cases (Fig. 1S, Supplementary Material). Comparison of these results with the data previously reported [23–27] for the analogous biogenic polyamines spermidine and spermine (Figs. 1S and 2S, Supplementary Material) allows a clear assignment of the features corresponding to their common molecular core (Tables 1–3): NH_2/NH_3 deformation modes at about 1600 cm^{-1}; intense features at *ca.* 1450–1500 cm^{-1} and 1200–1320 cm^{-1}, mainly assigned to CH_2 deformations (twisting and wagging respectively); strong signals predominantly due to NH_2/NH_3 deformations (also containing a contribution from CH_2 deformations), detected at *ca.* 1260 and 1200 cm^{-1} for the solid

Table 1
Main vibrational modes (cm^{-1}) for NSpd, Pt_3-$NSpd_2$ and Pd_3-$NSpd_2$.

NSpd			Pt_3-$NSpd_2$		Pd_3-$NSpd_2$		Approximate description
Exp.		Calc.[a]	Exp.		Exp.		
FTIR	Raman		FTIR	Raman	FTIR	Raman	
3362	3362	3442	3262	3267	3269	3283	$\nu_s(NH_3)$
3278	3302	3346	3248	3250	3224	3227	$\nu_s(NH_3)+\nu_s(NH_2)$
3187	3188	3220	3215	3219	3172	3172	$\nu_{as}(NH_3)+\nu_{as}(NH_2)$
		3217	3148	3152	3154	3158	$\nu_s(NH_2)$
2939	2955	3137	2942	2942	2939	2940	$\nu_{as}(CH_2)$
2905	2909		2877	2915	2874	2903	$\nu_{as}(CH_2)$
2852	2861		2854	2878	2846	2876	$\nu_s(CH_2)$
1600	1600		1608		1605		$\delta_{sciss}(NH_2)$
1466	1478	1470	1462	1459	1460	1459	$\delta_{sciss}(CH_2)$
1439	1444	1410	1446		1449		$\delta_{sciss}(CH_2)$
1365	1360						$\delta_{sciss}(CH_2)$
1307	1300	1252	1258		1249		$\delta_{sciss}(CH_2)+t(CH_2)$
			1172	1170	1171		$\omega(CH_2)+t(CH_2)$ $+\delta(NH_3)+\nu(CC)$
1126	1113	1186	1148		1146	1143	$\omega(CH_2)+t(CH_2)$ $+\delta(NH_3)+\nu(CC)$
1070	1070	1112	1064	1036	1053	1062	$\omega(CH_2)+t(CH_2)$
			1035		1031		$\omega(CH_2)+t(CH_2)$
979	980	1018					$\nu(CC)+\nu(CN)$
915	915	970					$t(CH_2)+\delta_s(NH_3)$ $+\delta_{sciss}(NH_2)+\nu(CC)$
884	865	906					$\delta_{sciss}(NH_2)+\omega(NH_2)$
843	841	880					$\delta_s(NH_3)$
766	772	766					$r(CH_2)+r(NH_3)+r(NH_2)$
557	554						$r(NH_3)$
			522	536 (524)[b]		522	ν_s(NMN)[c]
			483	482 (508)[b]	498	498	ν_{as}(NMN)
				391		388	ν(ClMCl)
				333 (323)[b]		340	ν_s(ClMCl)
				316 (317)[b]		307	ν_{as}(ClMCl)
	281						LAM[d]
				229 (255)[b]		225	δ(NMN)
				171 (162)[b]		173	δ(ClMCl)
	118						TAM[d]

[a] At the B3LYP/6-31G** level wavenumbers above 600 cm^{-1} are scaled by 0.9614 [41]. ν—Stretching; δ—in-plane deformation; t—twisting; r—rocking; ω—wagging; sciss—scissoring; s—symmetric; as—antisymmetric.
[b] From Ref. [31].
[c] M = Pt(II) or Pd(II).
[d] LAM and TAM refer to longitudinal and transverse acoustic modes, respectively.

Table 2
Main vibrational modes (cm^{-1}) for BENSpm and Pd_2-BENSpm.

BENSpm			Pd_2-BENSpm		Approximate description
Exp.		Calc.[a]	Exp.		
FTIR	Raman		FTIR	Raman	
3147	3167	3342	3221	3229	$\nu_s(NH_2)$
3123					$\nu_s(NH_2)$
3083	3031	3028			$\nu_{as}(CH_3)$
		3011			$\nu_{as}(CH_2)+\nu_{as}(CH_3)$
2989	2976	2975	2981	2992	$\nu_{as}(CH_2)$
2951	2932	2947	2971	2968	$\nu_s(CH_2)$
		2934			$\nu_s(CH_3)$
2927	2909	2923	2923	2923	$\nu_s(CH_2)$
2889	2881		2865	2865	$\nu\nu_s(CH_2)$
1635	1694		1625	1623	$\delta_{sciss}(NH_2)$
1596	1595	1623			$\delta_{sciss}(NH_2)+\delta_{sciss}(CH_2)$
1490	1488	1511			$\delta(CH_3)$
1461	1471	1500	1463	1455	$\omega(CH_2)+t(CH_2)+\omega(NH_2)+\delta(NH_2)$
1405	1437	1468	1439	1433	$\omega(CH_2)+t(CH_2)+\omega(NH_2)+\delta(NH_2)$
1394	1392	1456	1386	1388	$\delta_{sciss}(CH_2)+t(NH_2)$
1357		1405	1354	1355	$\delta_{sciss}(CH_2)+t(CH_2)+\omega(CH_2)$
	1312	1363	1306	1307	$\omega(CH_2)+t(CH_2)+t(NH_2)$
			1296	1293	$\omega(CH_2)+\omega(NH_2)+\delta(NH_2)$
1264	1257	1309	1281	1252	$\omega(CH_2)+t(CH_2)+t(NH_2)$
			1175	1178	$\omega(CH_2)+r(NH_2)$
1152	1149	1173	1146	1141	$\nu(CC)+\nu(CN)$
1050	1049	1084	1069	1074	$\nu(CC)+\nu(CN)$
1035	1035	1075	1038	1039	$\nu(CC)+\nu(CN)$
			1023	1014	$\nu(CC)+\nu(CN)$
999	999	1023	993	989	$\nu(CC)+\nu(CN)$
			966	936	$t(CH_2)+r(CH_2)+r(NH_2)$
906	884	931	892	887	$t(CH_2)+r(CH_2)+r(NH_2)$
			835	833	$r(NH_2)$
805	804	838	804	809	$r(CH_2)+r(NH_2)$
782	780	778	745	748	$r(CH_2)+r(NH_2)$
			697	700	$r(CH_2)$
				563	$\nu_s(NPdN)$
				505	$\nu_{as}(NPdN)$
				487	$\nu_{as}(NPdN)$
				424	$\nu_s(ClPdCl)$
				325	$\nu_{as}(ClPdCl)$
				295	$\delta(NPdN)$
				222	$\delta(ClMCl)$

[a] At the B3LYP/6-31G** level wavenumbers above 600 cm^{-1} are scaled by 0.9614 [41]. ν—Stretching; δ—in-plane deformation; t—twisting; r—rocking; ω—wagging; sciss—scissoring; s—symmetric; as—antisymmetric.

Table 3
Main vibrational modes (cm^{-1}) for CPENSpm and Pt_2-CPENSpm.

CPENSpm			Pt_2-CPENSpm		Approximate description
Exp.		Calc.[a]	Exp.		
FTIR	Raman		FTIR	Raman	
3129		3330	3139	3165	$\nu_{as}(NH_2)$
3072	3070	3228		3061	$\nu_s(NH_2)$
		3215			$\nu_{as}(CH_3)$
2973	2973	3231	2960	2995	$\nu_{as}(CH_2)$
2935	2934	3135	2937	2939	$\nu\nu_s(CH_2)$
	2907	3134			$\nu(CH)^{cyclop}$
		3121			$\nu_s(CH_3)$
2864	2878	2949	2879	2880	$\nu_s(CH_2)$
	2808	2885			$\nu(CH/CH_2)^{cyclop}$
1592			1608		$\delta_{sciss}(NH_2)$
1575	1577				$\delta_{sciss}(CH_2)+\delta_{sciss}(NH_2)$
1481	1485	1500			$\delta(CH_3)$
1452	1463		1465	1461	$\omega(CH_2)+t(CH_2)+\delta(NH_2)+\omega(NH_2)$
1408	1414	1477	1455	1451	$\delta_{sciss}(CH_2)$
1391	1385	1464	1386	1373	$\delta_{sciss}(CH_2)$
1355	1349	1391			$\delta_{sciss}(CH_2)+t(CH_2)$
	1314	1333	1320	1310	$\omega(CH_2)+t(CH_2)+t(NH_2)$
1263	1256	1289			$\omega(CH_2)+t(CH_2)+t(NH_2)$
1212	1201	1199	1191	1196	$\omega(CH_2)+t(CH_2)^{cyclop}+t(NH_2)$
1148	1147	1175	1159		$\omega(CH_2)+t(NH_2)$
1049	1048	1104	1048		$\nu(CC)+\nu(CN)$
1027		1033			$\nu\nu(CC)+\nu(CN)$
1000		1013			$\nu(CC)+\nu(CN)$
	884	920	878		$t(CH_2)+r(CH_2)+t(NH_2)+\omega(NH_2)$
830	833	858	834	831	$t(CH_2)+r(CH_2)+t(NH_2)$
800	802	807	808	810	$t(CH_2)^{cyclop}$
777	778	786	773	779	$r(CH_3)+r(NH_2)$
				516	$\nu_s(NPtN)$
				483	$\nu\nu_{as}(NPtN)$
				386	$\nu_s(ClPtCl)$
				368	$\nu_s(ClPtCl)$
				321	$\nu\nu_{as}(ClPtCl)$
	252				$\nu(CC)^{cyclop}$
				220	$\delta(NPtN)$
	216				LAM[b]
				197	$\delta(ClPtCl)$
				168	$\delta(ClPtCl)$

[a] At the B3LYP/6-31G** level wavenumbers above 600 cm^{-1} are scaled by 0.9614 [41]. ν—Stretching; δ—in-plane deformation; t—twisting; r—rocking; ω—wagging; sciss—scissoring; s—symmetric; as—antisymmetric.
[b] LAM refers to a longitudinal acoustic mode.

compounds (BENSpm and CPENSpm) and between 1113 and 1126 cm^{-1} for NSpd; the NH_2 rocking vibration, in turn, was observed at 745–970 cm^{-1} for the terminally alkylated polyamines, while for norspermidine a broad band, centred at 770 cm^{-1} was detected (particularly intense in infrared), encompassing both NH_2 and NH_3 rocking modes. For the alkylated molecules BENSpm and CPENSpm, a characteristic deformation mode of the terminal methyl group appears around 1480–1500 cm^{-1} (Tables 2 and 3). All the modified PA's presently studied are solids, except for NSpd which is a liquid at room temperature leading to an expected broadening of the FTIR and Raman signals (Fig. 2S, Supplementary Material).

The signals from the rocking deformations of the terminal NH_3 groups, clearly detected for NSpd at 841/843 cm^{-1} by both FTIR (very intense band) and Raman (Table 1), are absent in BENSpm and CPENSpm due to alkylation at these nitrogen atoms (Figs. 2 and 3), while the bands assigned to NH_2 symmetric and antisymmetric deformations are observed (as theoretically predicted) at *ca.* 1600 cm^{-1} for the three PA's. Although two calculated bands occur for these NH_2 (scissoring) vibrations, ascribed to either the two inner amine groups or the terminal ones, the experimental data do not allow to distinguish them. Moreover, the NSpd $r(NH_3)$ modes are particularly intense in the FTIR spectra, as compared to the corresponding Raman profile (Fig. 2S, Supplementary Material), as expected. Also, the NH stretching vibrations display a larger infrared intensity relative to their Raman activity when compared to the ν(CH) modes, for all the molecules studied.

Unlike NSpd, which differs from Spd solely in the shorter carbon chain between nitrogens (three carbon atoms instead of four in the natural PA), the spectra of BENSpm and CPENSpm vary from those of their biogenic counterpart (spermine) in the absence of the terminal $\delta(NH_2)$ mode at *ca.* 1600 cm^{-1}, due to the terminal alkylation of these amines. It is interesting to note that the Raman spectrum of norspermidine displays quite strong features due to the stretching of the terminal NH_3 groups, that are absent in the alkylated polyamines (for which the corresponding modes for the central NH_2 moieties are undetectable). Furthermore, the cyclopropyl-containing PA, CPENSpm, displays several bands characteristic from this group (Table 3): the CH_2 twisting modes, at 1201 cm^{-1}, quite intense in the Raman spectrum (Table 3) while hardly observed by infrared; methylene deformations at 800 cm^{-1}, present in both the FTIR and the Raman pattern (Fig. 3); and the ring C–C stretching, detected by Raman at 252 cm^{-1} (Fig. 1S, Supplementary Material). As opposed to norspermidine, the Raman bands corresponding to the amine stretching modes are not detected.

Some of the acoustic modes typical of this kind of *all-trans*, extended, molecules comprising repeating CH_2/NH_2 units [23,26] – either longitudinal (LAM's) or transverse (TAM's) – were detected in the Raman spectra presently obtained (Tables 1 and 3), namely the symmetric LAM1 (accordion mode) at 281 and 216 cm^{-1} for NSpd

and CPENSpm, respectively (Figs. 1S and 2S, Supplementary Material), and one of the lower frequency TAM's, observed for NSpd at 120 cm^{-1} (Fig. 2S, Supplementary Material). Additionally, NSpd and BENSpm being centrossymmetric species, a complementary infrared and Raman pattern was obtained, as opposed to their biogenic counterparts Spd and Spm [24,27].

The polyamine chelates presently studied vary in their coordination pattern, according to the type of ligand—either tri- or tetramine: in $(MCl_2)_3(NSpd)_2$ (M_3-$NSpd_2$) two of the metal ions are bound to each of the norspermidine ligands, while the third is shared by both amines. In $(PdCl_2)_2$(BENSpm) (Pd_2-BENSpm) and $(PtCl_2)_2$(CPENSpm) (Pt_2-CPENSpm), in turn, the two metal centres coordinate to the four nitrogens of the spermine-like molecule.

The spectroscopic data presently gathered corroborate this type of coordination, both Pt(II) and Pd(II) being known to have a significant affinity for nitrogen atoms. Upon metal binding, the vibrational pattern of the ligands undergo clear changes, such as the expected loss of the main bands assigned to the NH_2/NH_3 groups, namely $\delta(NH_2)$ around 1600 cm^{-1}, as well as $\rho(NH_3)$ (Figs. 2 and 3; 3S and 4S, Supplementary Material) (*e.g.* for NSpd, $\delta(NH_3)$ at *ca.* 555/770 cm^{-1} and $\delta(NH_3)$ at *ca.* 1120 cm^{-1}). Additionally, the NH stretching bands reflect the presence of the metal through a marked shift to higher frequencies, plainly detected by FTIR for the terminally alkylated ligands BENSpm and CPENSpm (Figs. 2(b) and 3(b))—ascribed to the change from $\nu(NH_2)/\nu(NH_3)$ symmetric and antisymmetric vibrations, in the free ligands, to the corresponding modes for the metal-coordinated amine groups. This is particularly evident in the Raman spectra of the terminally alkylated systems since the amine stretching features are hardly observable for the free ligands, but become quite intense for the corresponding complexes (Figs. 2(b) and 3(b)). For the non-alkylated polyamine NSpd, in turn, these features ($\nu(NH_2)/\nu(NH_3)$) are detected for both the complex and the uncoordinated molecule, undergoing a significant intensity decrease upon metal binding (Fig. 4S(b), Supplementary Material). Concomitantly, distinct new signals appear in the Raman pattern below *ca.* 600 cm^{-1}, characteristic of the metal coordination profile: deformations, between 165 and 225 cm^{-1} (δ(Cl–M–Cl)) and 220 to

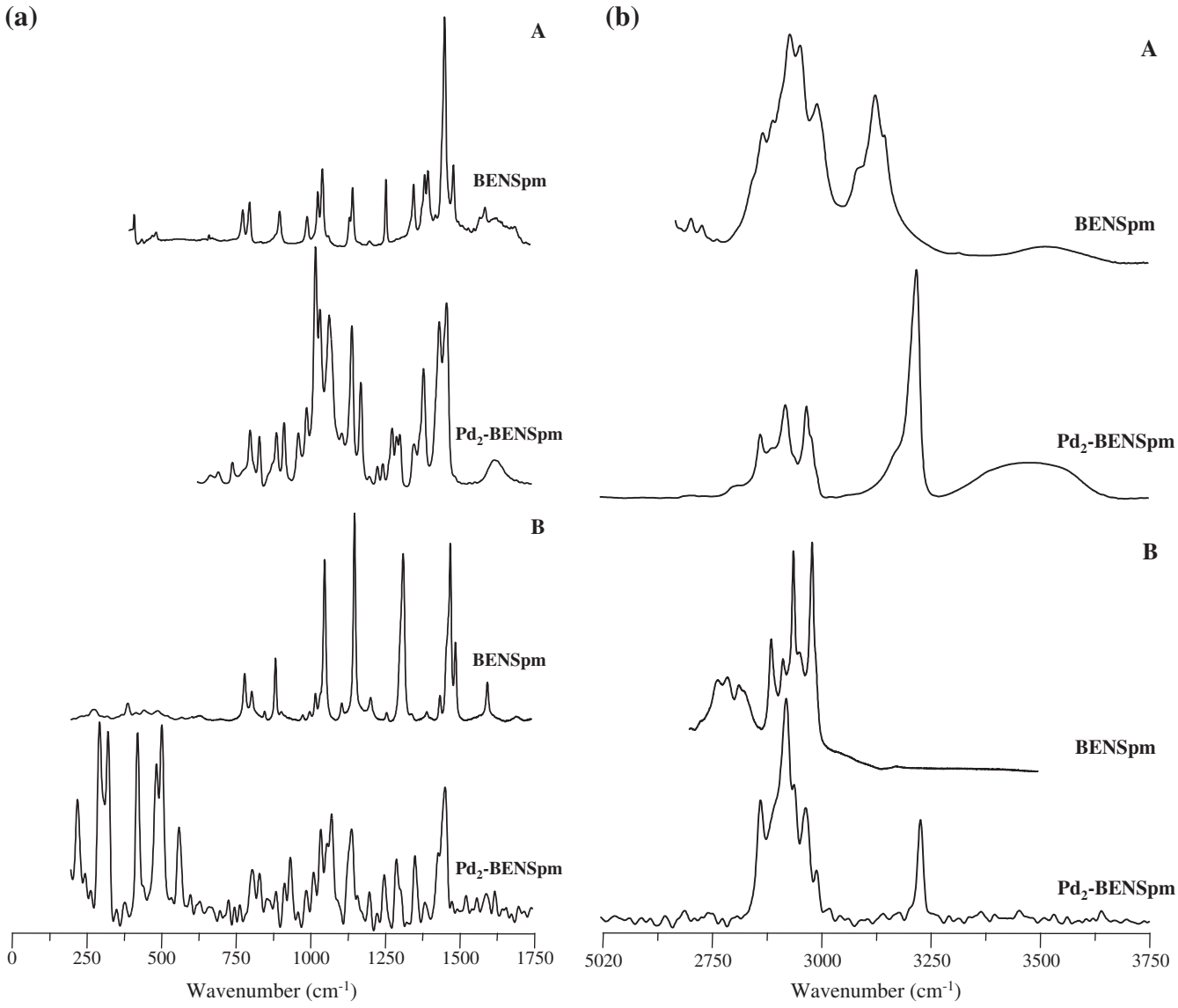

Fig. 2. Experimental FTIR (A) and Raman (B) spectra for BENSpm and Pd_2-BENSpm.

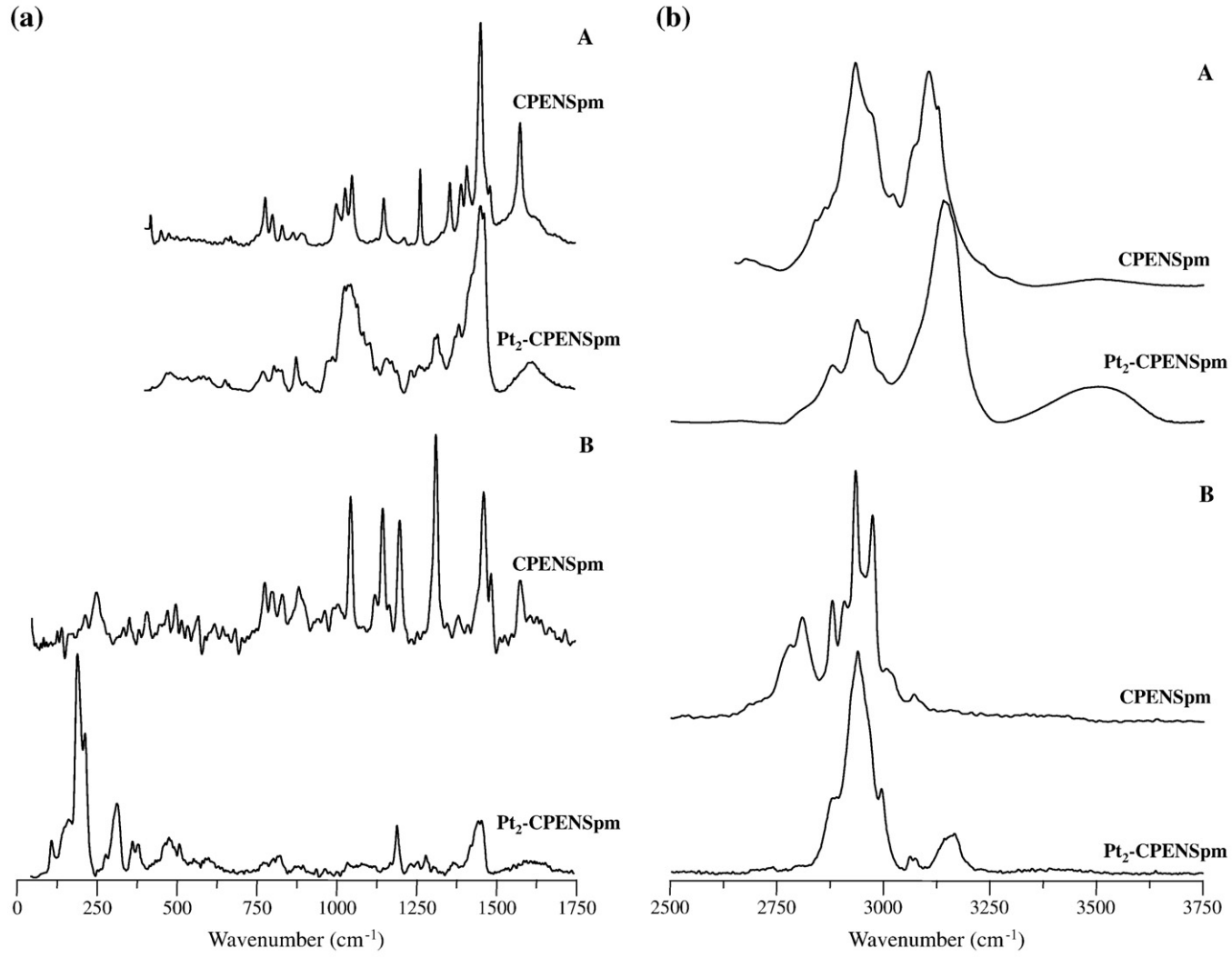

Fig. 3. Experimental FTIR (A) and Raman (B) spectra for CPENSpm and Pt_2-CPENSpm.

295 cm^{-1} (δ(N–M–N)), as well as symmetric and antisymmetric (Cl–M–Cl) and (N–M–N) stretching modes, between 305 to 425 cm^{-1} and 480 to 565 cm^{-1}, respectively (Tables 1–3). A Pd for Pt substitution (in the NSpd complexes) was found to lead to a change in the band profile assigned to the symmetric and antisymmetric (metal–N) stretching modes—either a broad feature or a well resolved two-band pattern in the 460–540 cm^{-1} interval (Figs. 3S and 4S, Supplementary Material). Overall, complexation of the polyamine ligands leads to a marked weakening of the Raman bands at higher wavenumbers (*ca.* above 1000 cm^{-1}) relative to the very intense signals that appear below *ca.* 600 cm^{-1}, which are due to strong vibrational modes involving the metal and its primary coordination sphere.

These results are in accordance with the previously gathered data for cisplatin and its Pd(II) homologue [28–31], as well as for the similar polynuclear spermidine (M_3-Spd_2) and spermine (M_2-Spm) chelates (M = Pt(II) or Pd(II)) [unpublished data]. Actually, comparison of the vibrational profile of the presently investigated cisplatin-like chelates, comprising two or three (MCl_2NH_2) moieties, with cisplatin's vibrational pattern [31] allows to conclude that the deformation and stretching modes involving the metal centre, either platinum(II) or palladium(II), occur in defined spectral regions irrespective of the type of species – either the mononuclear cisplatin and its Pd(II) homologue, or the di- and trinuclear polyamine chelates – since they reflect a very similar metal coordination sphere (Table 1).

4. Conclusions

Interference with polyamine homeostasis through administration of modified homologues, and the use of metal complexes with a view to affect cell growth *via* DNA covalent binding are promising therapeutic approaches against cancer. In order to follow this type of strategies, a thorough knowledge of the conformational preferences of both modified polyamines and their chelates is crucial for understanding the mechanisms through which they are transported into the cell (pharmacokinetics) and the molecular basis of their biological activity (pharmacodynamics).

The reported results allow to conclude on the success of the synthetic route followed for the preparation of the Pd(II) and Pt(II) chelates with modified biogenic polyamines (tri- and tetramines), presently modified and improved relative to previously published methods applied to Spd and Spm complexes. Additionally, the theoretical approach used to simulate these systems showed to be quite suitable, as expected in the light of previous data published by the authors on cisplatin and analogous complexes (*e.g.* with Pd(II)).

As expected, and similarly to the previously reported studies on biogenic polyamines, the *all-trans* geometry was found to be energetically favoured for all the alkylated linear amines presently investigated, considering their physiological, totally protonated, state. As to the corresponding polynuclear chelates, newly synthesised through dedicated

optimised routes, they display a stable geometry very similar to that previously obtained for their analogues with the biogenic PA's spermidine (M_3-Spd_2) and spermine (M_2-Spm), comprising two or three cisplatin-like (MCl_2NH_2) moieties. Therefore, when interacting with DNA (their main biological target) they are able to bind to the purine/pirimidine bases through two or three different sites simultaneously upon hydrolysis of the chloride atoms (long-range intra- and inter-strand interactions), which can greatly enhance their cytotoxicity over conventional, mononuclear, drugs such as cisplatin.

This type of conformational studies (both for the targets and the potential chemotherapeutic agents) is the basis for a rational development of new anticancer drugs, coupling a higher (and hopefully selective) cytotoxic activity to an optimised therapeutic efficacy, as well as to the capacity of overcoming resistance to clinically used agents. Concomitant biological studies – cytotoxicity and cell growth inhibition evaluation – are being performed for both the modified PA's and their Pt(II) and Pd(II) chelates in human cancer cell lines (*e.g.* breast cancer), aiming at linking structural preferences to anticancer effect, leading to the establishment of consistent structure–activity relationships (SAR's) for this kind of polyamine-based systems.

5. Abbreviations

Put	putrescine
Spd	spermidine
Spm	spermine
NSpd	norspermidine
BENSpm	N^1,N^{11}-bis(ethyl)norspermine
CPENSpm	N^1-cyclo-propylmethyl-N^{11}-ethylnorspermine
PA	polyamines
FTIR	Fourier transform infrared spectroscopy
MCT	mercury cadmium telluride
CCD	charge coupled device
DFT	density functional theory
HF	Hartree–Foch
rms	root-mean-square

Supplementary data to this article can be found online at doi:10.1016/j.jinorgbio.2011.11.021.

Acknowledgements

The authors thank the Chemistry Department of the University of Aveiro for use of the FT–Raman spectrometer. The authors acknowledge financial support from the Portuguese Foundation for Science and Technology-PEst-OE/QUI/UI0070/2011 and PhD fellowship SFRH/BD/46364/2008 (TMS). TMS is grateful for help regarding the synthetic procedure (Sónia Fiuza) and spectral analysis (Nelson Machado).

References

[1] K. Igarashi, K. Kashiwagi, Plant Physiol. Biochem. 48 (2010) 506–512.
[2] E. Agostinelli, M.P. Marques, R. Calheiros, F.P. Gil, G. Tempera, N. Viceconte, V. Battaglia, S. Grancara, A. Toninello, Amino Acids 38 (2010) 393–403.
[3] A. Onal, Crit. Rev. Anal. Chem. 40 (2010) 60–67.
[4] K. Dredge, J.A. Kink, R.M. Johnson, I. Bytheway, L.J. Marton, Cancer Chemother. Pharmacol. 65 (2009) 191–195.
[5] N. Seiler, Curr. Drug Targets 4 (2003) 565–585.
[6] R.A. Casero, P.M. Woster, J. Med. Chem. 52 (2009) 4551–4573.
[7] R.A. Casero, P.M. Woster, J. Med. Chem. 44 (2001) 1–26.
[8] Y. Huang, A. Pledgie, R.A. Casero Jr., N.E. Davidson, Anticancer Drugs 16 (2005) 229–241.
[9] A.C. Wolff, D.K. Armstrong, J.H. Fetting, M.K. Carducci, C.D. Riley, J.F. Bender, R.A. Casero Jr., N.E. Davidson, Clin. Cancer Res. 9 (2003) 5922–5928.
[10] Pledgie-Tracy, M. Billam, A. Hacker, M.D. Sobolewski, P.M. Woster, Z. Zhang, R.A. Casero, N.E. Davidson, Cancer Chemother. Pharmacol. 65 (2010) 1067–1081.
[11] K. Chválová, J. Kaspárková, N. Farrell, V. Brabec, FEBS J. 273 (2006) 3467–3478.
[12] S. Komeda, T. Moulaei, M. Chikuma, A. Odani, R. Kipping, N. Farrell, L.D. Williams, Nucleic Acids Res. (2010) 1–12.
[13] M.P. Marques, T. Girão, M.C. Pedroso de Lima, A. Gameiro, E. Pereira, P. Garcia, Biochim. Biophys. Acta-MCR 1589 (2002) 63–70.
[14] L.J. Teixeira, M. Seabra, E. Reis, M.T. da Cruz, M.C. de Lima, E. Pereira, M.A. Miranda, M.P. Marques, J. Med. Chem. 47 (2004) 2917–2925.
[15] S.M. Fiuza, A.M. Amado, Paulo J. Oliveira, Vilma A. Sardão, L.A.E. Batista de Carvalho, M.P. Marques, Lett. Drug Des. Discov. 3 (2006) 149–151.
[16] A.S. Soares, S.M. Fiuza, M.J. Gonçalves, L.A.E. Batista de Carvalho, M.P. Marques, A.M. Urbano, Lett. Drug Des. Discov. 4 (2007) 460–463.
[17] R. Tummala, P. Diegelman, S.M. Fiuza, L.A.E. Batista de Carvalho, M.P. Marques, D.L. Kramer, K. Clark, S. Vujcic, C.W. Porter, L. Pendyala, Oncol. Rep. 24 (2010) 15–24.
[18] A. Tassoni, N. Bagni, M. Ferri, M. Franceschetti, A. Khomutov, M.P. Marques, S.M. Fiuza, A.R. Simonian, D. Serafini-Fracassini, Plant Physiol. Biochem. 48 (2010) 496–505.
[19] O. Corduneanu, A.M. Chiorcea-Paquim, S.M. Fiuza, M.P. Marques, A.M. Oliveira-Brett, Bioelectrochemistry 78 (2010) 97–105.
[20] O. Corduneanu, A.M. Chiorcea-Paquim, V. Diculescu, S.M. Fiuza, M.P. Marques, A.M. Oliveira-Brett, Anal. Chem. 82 (2010) 1245–1252.
[21] S.M. Fiuza, J. Holy, L.A.E. Batista de Carvalho, M.P. Marques, Chem. Biol. Drug Des. 77 (2011) 477–488.
[22] A.M. Amorim da Costa, M.P. Marques, L.A.E. Batista de Carvalho, Vib. Spec. 29 (2002) 61–67.
[23] M.P. Marques, L.A.E. Batista de Carvalho, J. Tomkinson, J. Phys. Chem. A 106 (2002) 2473–2482.
[24] A.M. Amorim da Costa, M.P. Marques, L.A.E. Batista de Carvalho, J. Raman Spectrosc. 34 (2003) 357–366.
[25] A.M. Amorim da Costa, L.A.E. Batista de Carvalho, M.P.M. Marques, Vib. Spec. 35 (2004) 165–171.
[26] L.A.E. Batista de Carvalho, M.P. Marques, J. Tomkinson, J. Phys. Chem. A 110 (2006) 12947–12954.
[27] M.P. Marques, L.A.E. Batista de Carvalho, Biochem. Soc. Trans. 35 (2007) 374–380.
[28] A.M. Amado, S.M. Fiuza, M.P. Marques, L.A.E. Batista de Carvalho, J. Chem. Phys. 127 (2007) 185104–185110.
[29] S.M. Fiuza, A.M. Amado, M.P. Marques, L.A.E. Batista de Carvalho, J. Phys. Chem. A 112 (2008) 3253–3259.
[30] S.M. Fiuza, A.M. Amado, H.F. dos Santos, M.P. Marques, L.A.E. Batista de Carvalho, Phys. Chem. Chem. Phys. 12 (2010) 14309–14321.
[31] L.A.E. Batista de Carvalho, M.P. Marques, C. Martin, S.F. Parker, J. Tomkinson, Chem. Phys. Chem. 12 (2011) 1334–1341.
[32] C. Navarro-Ranninger, P.A. Ochoa, J.M. Pérez, V.M. González, J.R. Masaguer, C. Alonso, J. Inorg. Biochem. 53 (1994) 177–190.
[33] G. Codina, A. Caubet, C. Lopez, V. Moreno, E. Molins, Helv. Chim. Acta 82 (1999) 1025–1037.
[34] M.J. Frisch, G.W. Trucks, H.B. Schlegel, G.E. Scuseria, M.A. Robb, J.R. Cheeseman, J.A. Montgomery Jr., T. Vreven, K.N. Kudin, J.C. Burant, J.M. Millam, S.S. Iyengar, J. Tomasi, V. Barone, B. Mennucci, M. Cossi, G. Scalmani, N. Rega, G.A. Petersson, H. Nakatsuji, M. Hada, M. Ehara, K. Toyota, R. Fukuda, J. Hasegawa, M. Ishida, T. Nakajima, Y. Honda, O. Kitao, H. Nakai, M. Klene, X. Li, J.E. Knox, H.P. Hratchian, J.B. Cross, V. Bakken, C. Adamo, J. Jaramillo, R. Gomperts, R.E. Stratmann, O. Yazyev, A.J. Austin, R. Cammi, C. Pomelli, J. Ochterski, P.Y. Ayala, K. Morokuma, G.A. Voth, P. Salvador, J.J. Dannenberg, V.G. Zakrzewski, S. Dapprich, A.D. Daniels, M.C. Strain, O. Farkas, D.K. Malick, A.D. Rabuck, K. Raghavachari, J.B. Foresman, J.V. Ortiz, Q. Cui, A.G. Baboul, S. Clifford, J. Cioslowski, B.B. Stefanov, G. Liu, A. Liashenko, P. Piskorz, I. Komaromi, R.L. Martin, D.J. Fox, T. Keith, M.A. Al-Laham, C.Y. Peng, A. Nanayakkara, M. Challacombe, P.M.W. Gill, B.G. Johnson, W. Chen, M.W. Wong, C. Gonzalez, J.A. Pople, G. GAUSSIAN 03, Revision D.01 Gaussian, Inc., Wallingford, CT, 2004.
[35] C. Lee, W. Yang, R.G. Parr, Phys. Rev. B 37 (1988) 785.
[36] B. Miehlich, A. Savin, H. Stoll, H. Preuss, Chem. Phys. Lett. 157 (1989) 200–206.
[37] A.D. Becke, Phys. Rev. A 38 (1988) 3098–3100.
[38] A.D. Becke, J. Chem. Phys. 98 (1993) 5648–5652.
[39] G.A. Petersson, A. Bennett, T.G. Tensfeldt, M.A. Al-Laham, W.A. Shirley, J. Mantzaris, J. Chem. Phys. 89 (1988) 2193.
[40] C. Peng, P.Y. Ayala, H.B. Schlegel, M.J. Frisch, J. Comput. Chem. 17 (1996) 49.
[41] J.P. Merrick, D. Moran, L. Radom, J. Phys. Chem. A 111 (2007) 11683–11700.
[42] L.A.E. Batista de Carvalho, L.E. Lourenço, M.P. Marques, J. Mol. Struct. 639 (1999) 482–483.